Pergamon

Int. J. Heat Mass Transfer. Vol. 41, No. 16, pp. 2503–2515, 1998

Printed in Great Britain
0017–9310/98 $19.00+0.00

PII: S0017–9310(97)00316–5

Combustion of unsupported water-in-*n*-heptane emulsion droplets in a convection-free environment

G. S. JACKSON† and C. T. AVEDISIAN‡

Sibley School of Mechanical and Aerospace Engineering, Cornell University, Ithaca, NY 14853-7501 U.S.A.

(*Received* 10 *October* 1996 *and in final form* 1 *October* 1997)

Abstract—Results of an experimental study are reported for combustion of unsupported *n*-heptane droplets emulsified with water burning while levitated in microgravity where the effects of external convection are negligible. The results are compared to a pure heptane droplet and a mixture of two miscible liquids (methanol/dodecanol) burning under similar low convection conditions. The effect of water concentration on flame luminosity and sooting tendency, preferential vaporization of the emulsion components, and the role of the emulsifying agent in promoting disruptive burning were examined. The photographs showed less sooting for the emulsions relative to pure heptane, and a preferential vaporization process was revealed from the image analysis by an abrupt change in the vaporization rate. A period exists near the end of burning during which the droplet diameter is nearly constant, followed by a disruptive burning event. A quasi-steady complex chemistry analysis with variable properties shows that a frozen evaporation mode occurs after an initial delay period during which heptane is evaporating from the droplet. Predicted and measured burning rates are in good agreement during this later period.

1. INTRODUCTION

Water mixed with an immiscible hydrocarbon droplet can have both beneficial and detrimental effects on the droplet combustion process. Water is known to reduce soot formation and radiation heat transfer to combustor walls [1], reduce flame temperatures and NO_x emissions [2], promote secondary droplet atomization or "microexplosion" [3] and encourage early flame extinction. Some of these effects are derived from water vapor being present on the fuel rich side of the flame that can only be achieved by emulsification of fuel with water compared to separate water injection [4].

In this paper we report the first results of an experimental study on combustion of near stationary and unsupported water-in-*n*-heptane emulsion droplets in a low gravity environment at atmospheric pressure to promote spherical symmetry in the burning process. The results are used to determine the emulsion droplet burning mode and to qualitatively examine the sooting propensity as water content is increased. Water is selected as the dispersed phase because of the aforementioned effects it can have on the burning process. Heptane (C_7H_{16}) is selected as the fuel phase to reference the results of water addition to prior work on heptane (0% water) droplet combustion in microgravity at atmospheric pressure [5]. Water emulsions with heavier *n*-alkanes proved too difficult to ignite using the spark ignition arrangement described in Section 2.

The advantage that combustion in a low convection environment brings to furthering the understanding of emulsion droplet combustion processes is to promote spherical symmetry. With no shear force at the droplet surface, streamlines of the flow are radial and the flame and droplet are concentric. Analysis of such complex phenomena as soot formation and detailed chemistry at the flame is facilitated by the resulting one-dimensional transport process. For the case of emulsion droplets, published models have assumed spherical symmetry so that data obtained for this condition can potentially be used to test the available theories.

Combustion of emulsified fuel droplets has been studied for many years and research on this subject continues to the present time. Spherical symmetry has been a goal of some of this work. Low gravity or low pressure has been used to reduce buoyancy, and all such studies in these environments employed emulsion droplets supported by fibers [2, 6–9]. A low pressure environment reduces sooting tendencies and can alter combustion chemistry and promote early extinction. Atmospheric (or higher) pressure combustion is more practical but must be carried out in a low gravity environment to realize spherical symmetry, or by using particularly small droplets ($< 100\ \mu m$) that can

† Currently Assistant Professor, Department of Mechanical Engineering, University of Maryland, College Park, MD 20742, U.S.A.

‡ Corresponding author.

NOMENCLATURE

C_D	laminar drag coefficient for a sphere	t	time.
D	droplet diameter		
D_o	initial droplet diameter	Greek symbols	
K	burning rate ($\equiv -d[D]^2/dt$)	μ_{air}	air viscosity (evaluated at 373 K)
Re	Reynolds number ($\equiv VD_o\rho_{air}/\mu_{air}$)	μ_l	emulsion viscosity
V	relative velocity between droplet and gas	ρ_{air}	air density (evaluated at 373 K)
		ρ_l	emulsion liquid density.

be difficult to optically resolve. The fiber support technique which is used to anchor the droplet can offer minimal disturbance to the burning process for single component and nonsooting fuels if the fiber diameter is small relative to the droplet diameter. However, additional factors make the fiber-supported technique inappropriate for emulsions: the potential for microexplosions (by heterogeneous bubble nucleation on the surface of the fiber) and coalescence of the dispersed phase. Unsupported droplets in these environments avoid these problems but pose special challenges when low gravity is used to reduce buoyancy for combustion in atmospheric pressure air.

Two limiting modes for emulsion droplet combustion are "distillation" and "frozen" [2]. In the distillation model the emulsion droplet composition is spatially uniform but varies with time. Vaporization is in the order of the volatility differential between the continuous (fuel) and dispersed (water) phases. Rapid mixing within the droplet is assumed. The frozen combustion mode assumes that the droplet is both spatially and temporally uniform and the vaporization of the dispersed phase occurs only when it is exposed by the regressing surface. For the frozen mode, vaporization is in the order of the liquid phase composition. The distillation mode is best realized when internal liquid motion provides rapid mixing inside the droplet. The frozen mode is plausible when there is no liquid motion.

The measurements we use to reveal which of these two combustion modes is operative is the evolution of droplet diameter, specifically the so-called "burning rate", $K = -d[D]^2/dt$. In frozen combustion, K should have one value throughout burning since both components vaporize together in the order of their liquid phase fractions throughout the burning process. For the distillation mode to be evidenced, the evolution of diameter would exhibit a "staged" process with K being determined by the dominant vaporizing component.

2. DESCRIPTION OF THE EXPERIMENT

The experimental design for studying combustion of free or unsupported emulsion droplets requires that the droplet be formed, deployed, positioned and held reasonably motionless within the focal plane of the camera, and (for the present study) in a low buoyancy environment. The emulsion components must not separate during the deployment and ignition process. Coalescence of the dispersed water microdroplets during the formation, deployment and combustion phases should be minimal.

A prior experimental design [5, 10–12] for studying combustion of unsupported fuel droplets in low buoyancy was adapted to study emulsion droplets. The experiment works as follows. A test emulsion droplet is propelled in a near vertical trajectory within a confined chamber (room temperature air in the present study) and then the combustion chamber with attached cameras and lighting are released into free fall (in a "drop tower") when the droplet reaches the apex of its trajectory. If the release of the package is properly timed, the chamber, cameras, and downwardly moving droplet fall at the same rate and appear motionless with respect to each other. The difficulty of perfectly timing the package release with the downward flight of the droplet often results in some motion of the droplet relative to the camera. This motion is small enough that the droplet flame is reasonably spherical and concentric with the droplet (as shown by the set of photographs discussed in Section 4).

Gravity levels in our experiment were less than 10^{-4} of Earth's normal gravity, achieved by placing a shield (a "drag" shield) around the falling package so that one package falls freely within another. The Grashof number for droplets of diameters of interest here is calculated to be less than 10^{-4} for which near spherical flames are realized [11]. The free-fall distance in the drop tower we used was long enough to create a period of observation (about 1.25 s) that was sufficient to observe the complete burning history for emulsion droplets with the initial diameters examined, between 0.58 mm and 0.74 mm. Reasonably clear photographs of the burning process are obtained for droplets of this size.

The ability to time the release of the package with the droplet reaching precisely the apex is dependent on knowing the trajectory height, the time it takes the droplet to reach it, and the delay time for the instrumentation package to separate from the electromagnet. Difficulties were experienced in achieving

the required degree of repeatability of the droplet trajectory for the water/heptane emulsions examined using our droplet generator (based on the ink-jet method [10]). This fact limited the number of successful observations of the burning process. The difficulties were believed to be due to the presence of the surfactant and water microdroplets within the droplet which influence both the effective viscosity of the emulsion and the surface tension. Results are presented in Section 4 for the most successful observations as determined by the clarity of the photographic image and the small motion of the droplet within the field of view for a significant fraction of its burning history.

Data acquisition was from a high speed 16 mm cine camera (LOCAM) with attached 90 mm/f2 Olympus Macro Lens. The movies provide qualitative information of flame luminosity and soot formation, as well as quantitative information on the evolution of droplet diameter and burning rates. More quantitative soot detection instrumentation (e.g., laser based methods) was not used for the free floating droplets because of the challenges inherent with eliminating completely movement of the droplet burning. Anchoring the droplet with a fiber to eliminate this problem was not an option for reasons stated previously, in addition to the fiber's tendency to attract soot particles. The initial droplet diameter, and room temperature atmospheric pressure conditions, were fixed while the water content in the emulsion droplets was varied.

Camera framing rates ranged from 100 frames s^{-1} to 400 frames s^{-1}. Measurements of droplet diameter were made from a frame-by-frame analysis using a computer-based image analysis system (Image Analyst™, Automatix Inc., Billerica, MA). The image analysis calculated an average diameter for the droplet, first by finding a perimeter for the droplet with a threshold gray level which was set by the operator according to the background of the film around the droplet, and then by averaging the distances from the perimeter to the center of mass for each pixel on the boundary. Errors, including calibration errors, resulted in no more than 2.0% for the droplet diameter measurements.

Ignition of the emulsion drops was via two sparks across two electrode pairs (of 200 μm diameter) positioned at the apex of the droplet trajectory. The two sparks are positioned on opposite sides of the drop to provide a breaking action to the droplet's motion and to promote more spherical ignition. Spark ignition is preferred because of the localized heating it provides to the surrounding gas with minimal disturbance. However, because of the sensitivity of the spherically symmetric burning process for sooting fuels to the ignition process, comparison of results from among studies that use different means of ignition is uncertain. The comparisons with pure heptane and a miscible mixture of methanol and dodecanol that are discussed in Section 4 use data obtained from the same apparatus as reported here [5, 12] with modifications being to the spark circuitry and electrode retraction mechanism.

The amount and duration of the spark energy was controlled in the present study. Spark energies and durations of about 0.09 J and 0.7 ms, respectively, were used for the emulsion droplets. For pure heptane (0% water), the spark duration and energy were 0.5 ms and 0.054 J, respectively.

The choice of emulsion mixture fractions tested was determined in part by the ability to ignite the droplets, and coping with the unsteadiness of the droplet stream noted previously. It was difficult to spark-ignite water/heptane emulsion droplets using our spark arrangement with water content greater than about 40%. For this reason, lower water volume fractions were selected: 10% and 30%. This limited range of water concentration was nonetheless sufficient to reveal insights and quantitative data of the emulsion droplet burning process at low gravity.

After ignition, the electrodes were retracted radially to provide an unobstructed ambience around the droplet flame. The electrode retraction was from miniature solenoids which we fabricated and wound by hand in our laboratory. Because high energy sparks provide an impulse to a free-floating droplet which can push it out of the camera's field of view, low boiling point and easily ignited fuel was selected as the continuous fuel phase in the present study. Asymmetries in the burning process (e.g., nonspherical flame shape) were observed immediately after ignition but quickly vanished (within 2 ms for a burning process that is longer than 500 ms) and gave way to reasonably spherical flames within 1% of the total droplet burning time for the cases reported here.

Since the droplets are formed at one location (the nozzle exit) and move to another (the apex) where they are ignited, the potential exists for internal circulation to occur in the droplet due to this motion which can influence the burning process. The primary transport effect of internal liquid circulation is to alter the geometry, and length and time scales associated with heat transfer within the droplet [13] which can affect the burning rate, extinction diameter and microexplosion. We cannot predict how the method of forming a droplet induces internal liquid circulation; it is better observed experimentally. The strength of internal circulation due to droplet motion can be estimated by comparing the characteristic time for circulation, and the decay time of its energy, to the droplet burning time.

The characteristic time (t_b) for droplet burning is D_o^2/K. We take the characteristic time for liquid motion (t_m) as the time for a particle to traverse the droplet circumference, which is approximately μ_l/τ_v assuming that the shear is continuous across the gas/liquid interface. In terms of the drag coefficient, $t_m \approx 2\mu_l/(\rho_{air} V^2 C_D)$. Defining a Reynolds number as $Re \equiv VD_o\rho_{air}/\mu_{air}$, then

$$\frac{t_m}{t_b} \approx \frac{2}{Re^2 C_D}\left(\frac{K\rho_{air}\mu_l}{\mu_{air}^2}\right).$$

An approximate emulsion viscosity is estimated from the formulations given by Pal and Rhodes [14], and a mean liquid density between water and heptane is used (i.e., $\mu_l \approx 4.95 \times 10^{-4}$ kg/(s-m), $\rho_l \approx 680$ kg/m^3) with water and heptane properties taken from Vargaftik [15]. For typical hydrocarbon fuels, $K \approx 10^{-6}$ m^2/s at atmospheric pressure. Using a laminar drag coefficient [16], and assuming for an extreme case that the source of circulation is due to the movement of the droplet from the nozzle exit to the apex for which $Re \approx 20$ at the nozzle exit in our experiment, then $t_m/t_b > 0.004$. Thus, internal circulation could be present within the droplet moving with $Re \approx 20$ when it is ignited. If the moving droplet is now suddenly stopped, which simulates the ideal condition of a droplet at the apex just prior to ignition when the instrumentation package is dropped, the fraction (ζ) of the total burning time for the energy of the circulating liquid motion to decay is estimated [17] to be $\zeta \approx 0.02K\rho_l/\mu_l$ if a linear decay of the energy of circulation is assumed. For the property values given above, $\zeta \approx 0.03$, which implies a decay of the circulation energy within 3% of the total burning time.

The gas phase symmetry is revealed by the shape of the flame and the soot shell. This symmetry indicates that the radial gas phase velocity component created by the evaporation process seems to dominate the flow field as evidenced by the reasonably spherical flames for most conditions as shown in Section 4.2. Internal circulation could affect extinction and the tendency for microexplosion. The former was not observed in our experiments while the latter effect is more likely rooted in the influence of the surfactant as discussed in Section 4.4.

3. PREPARATION OF EMULSIONS

The emulsions were prepared by combining the components in a beaker and dispersing them by agitation in an ultrasonic mixer. An emulsifying agent (a mixture of Span 80 and Tween 80) was added during agitation so that its total volume fraction in the emulsion was about 3% by volume based on previous studies [19, 20]. The composition of the emulsions discussed in this paper are the following: 87% heptane, 10% water and 3% surfactant for the emulsion labeled "10%" water; 68% heptane, 29% water, and 3% emulsifier by volume for the emulsion labeled "30%" water.

The emulsion structure was examined under a microscope. Macroscopically, the emulsions were milky white in appearance (e.g., [19]). Increasing the water concentration gave a much creamier appearance due to the higher density of water microdroplets. A rough estimate of the water microdroplet diameters indicated they had diameters on the order of a few microns with a range spanning about one order of magnitude.

The emulsions stored in the reservoir supplying the generator were stable during an experiment, in that the micron-sized water globules did not coalesce but rather remained dispersed during the flight of the test droplet to the apex of its trajectory. This was shown by collecting on a microscope cover glass emulsion droplets ejected from the droplet generator after 1 h of steady operation, examining them under a microscope, and then comparing the observations with samples of a freshly prepared emulsion that had not passed through the droplet generator. No visible changes in the emulsion structure were observed. Fresh emulsions were always made just before a group of experimental runs was performed.

4. EXPERIMENTAL RESULTS

4.1. *Evolution of droplet diameter*

The evolution of diameter for emulsion droplets containing 10% (by volume) and 30% (by volume) water is shown in Figs. 1 and 2, respectively (the lines shown on these Figures are predictions from an analysis that are discussed in Section 5). Shown also for comparison in Fig. 2 for the 30% water emulsion are data for a pure heptane droplet (0% water, $D_o \approx 0.69$ mm) previously reported [5] using the experimental technique described in Section 2. The ordinate is the droplet diameter divided by the initial droplet diameter, and the abscissa is a scaled time, t/D_o^2. The reason for presenting the results in this way is derived from the "D-squared" law (e.g., [21]) result according to which

$$\left(\frac{D}{D_o}\right)^2 = 1 - K\left(\frac{t}{D_o^2}\right) \quad (1)$$

If the burning rate is constant and the ratio of droplet to flame diameter is also constant (D/D_f = constant), then the burning process is termed "quasi-steady". The luminous part of the emulsion flames were too faint for the lighting used for accurate measurement of the flame boundary, and no flame diameter measurements are reported.

The period of observation for 30% water (Fig. 2) is terminated at $t/D_o^2 \approx 1.3$ s/mm^2 due to excessive drift of the droplets which affected image clarity and the ability to accurately measure droplet diameter. The droplets could, though, still be discerned by eye from the high speed film record and the dotted line with the star at the end of Fig. 2 is the trend that is believed to best represent the evolution of diameter during this period for this water concentration. For the 10% water emulsions (Fig. 1), at $t/D_o^2 > 1.3$ s/mm^2 a microexplosion event occurs that is also indicated by the "starred" point ("*").

The results of measuring the evolution of droplet diameter show the following: the burning rate is reduced as the water content increases; and a staged

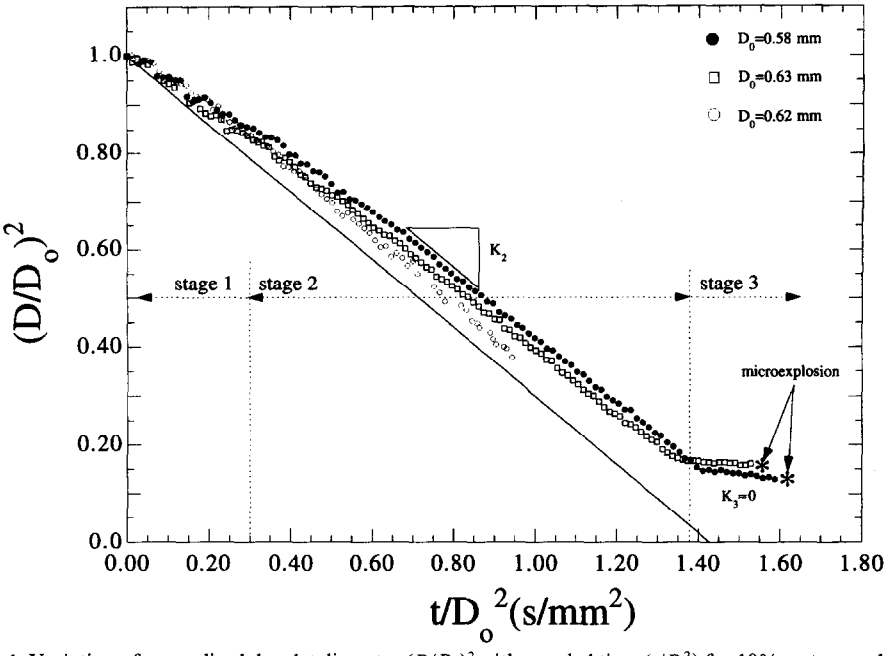

Fig. 1. Variation of normalized droplet diameter $(D/D_o)^2$ with a scaled time (t/D_o^2) for 10% water emulsion droplets. Inset indicates initial droplet diameters. Various stages are indicated by the dashed lines. Solid line is a prediction from the numerical analysis. Stage 3 is dominated by surfactant vaporization and terminates in a disruptive burning event.

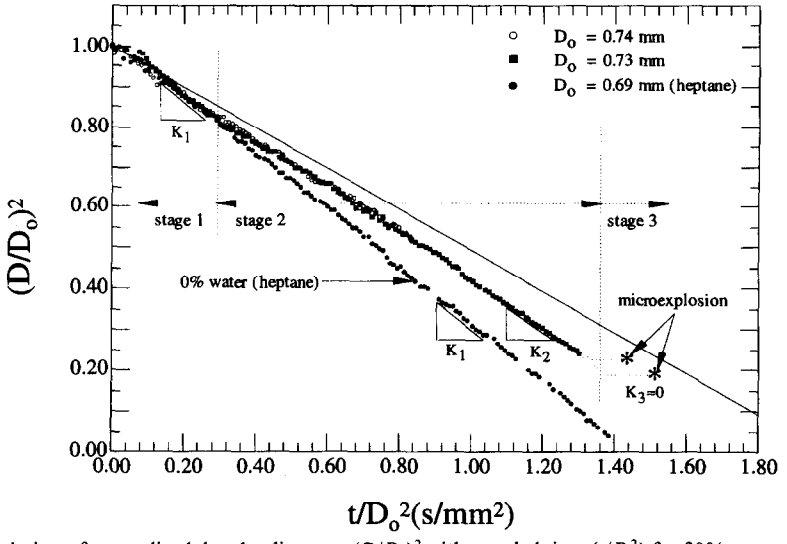

Fig. 2. Variation of normalized droplet diameter $(D/D_o)^2$ with a scaled time (t/D_o^2) for 30% water emulsion droplets. Inset indicates initial droplet diameters. Shown for comparison is the burning history of a pure heptane (0% water) droplet. Various stages are indicated by the dashed lines. Solid line is a prediction from the numerical analysis. Film image quality for stage 3 burning was not high enough for data analysis but visual inspection showed a disruptive burning event.

burning process is revealed for the 30% water emulsion during which K has a (nearly) unique value in various time domains of the burning process. Though the first stage boundary, "stage 1", is not clearly delineated for the 10% water data in Fig. 1, it is still indicated because the data seem to show a trend that suggests placement of this boundary, though it is not as obvious as for the 30% water data of Fig. 2.

The first stage indicated in Fig. 2 for the 30% emulsion droplets for $t/D_o^2 < 0.3$ s/mm^2 shows a burning rate ($\equiv K_1$) that is almost the same as for pure heptane. Stage 1, therefore, appears to be dominated by hep-

tane vaporization. For $0.3\ s/mm^2 < t/D_o^2 < 1.3\ s/mm^2$ the burning rate ($=K_2$) is slightly smaller than K_1 for the 30% emulsion which shows the effect of water vaporization. For the 10% emulsion with $D_o = 0.58$ mm (Fig. 1), K_1 was 10% higher than the other two emulsion droplets of this water content, and this may have been due to increased drift of this droplet which was evidenced in the high speed movie record for this droplet.

For stage 1, the burning rates averaged $0.68\ mm^2/s$ with an uncertainty of $\pm 0.06\ mm^2/s$. This value falls within the uncertainty range [5] of similarly-sized heptane droplets ($0.70 \pm 0.04\ mm^2/s$), which again suggests that heptane vaporization dominates stage 1 for the 30% water emulsion droplets. State 2 burning rates for the 10% water emulsion droplets (Fig. 2) averaged $0.56 \pm 0.02\ mm^2/s$ which is substantially lower than for pure heptane. For the 10% water emulsion droplets, the lowered burning rates between stages 1 and 2 are not clearly observed as shown in Fig. 2. With 10% water in the emulsion the difference in stage 1 and 2 burning rates which is clearly observed for the 30% water droplets apparently decreases for the 10% emulsions to below the limit of the data analysis to detect a difference in burning rates.

If the boundary between stages occurs between a low boiling point liquid and a high boiling point liquid, then the increase of droplet temperature as the higher boiling point species takes over lowers the liquid density and results in a period where the droplet diameter is nearly constant. This situation appears to be realized on the transition between stages 2 and 3 for the emulsion droplets (more clearly shown for 10% water) because of the large difference in boiling points between water or heptane and the emulsifying agent. However, since water and heptane have similar boiling points, thermal expansion effects are not significant during the transition between stages 1 and 2, so that the change in burning rates occurs abruptly between stages 1 and 2. A similar abrupt transition was observed during Leidenfrost evaporation of water/heptane emulsion droplets at a hot surface [19].

This staged burning process for a free emulsion droplet in microgravity is similar to that observed for burning a binary *miscible* mixture containing components with large differences in their volatility, which further illustrates the aforementioned effect of thermal expansion on the transition between stages. Figure 3 shows the evolution of diameter for an unsupported mixture droplet initially containing 25% (by volume) dodecanol in 75% methanol using the experimental arrangement discussed in Section 2. A transition period is seen for $0.55\ s/mm^2 < t/D_o^2 < 0.65\ s/mm^2$ where the diameter is nearly constant—note the dotted line in Fig. 3 ($K_2 \approx 0$)—because of thermal expansion during the transition associated with the differing boiling points between methanol (65°C) and dodecanol (259°C).

Flame boundaries for the emulsion droplet were too faint for quantitative measurement of their diameters for the image analysis system used. Close inspection of the video camera records showed luminous zone boundaries moving inward toward the droplet late in the burning process during the period where the droplet diameter was almost constant (stage 3 in Figs. 1 and 2). This behavior is attributed to enrichment of emulsifier concentration and to reduced vaporization as burning progresses. The phenomenon of shrinking flames which accompanies a change in the dominant vaporizing species, here from heptane and water to surfactant, is similar to that observed for miscible mixture droplets [2]. Shrinking flames for the water/heptane emulsion droplets signify reduced vaporization. Heat from the flame is largely being used to heat the droplet surface which has become enriched in the emulsifier concentration. Eventually, either the flame will extinguish if surfactant vapors cannot sustain combustion, or the droplet may microexplode if the droplet temperature increases substantially.

4.2. *Soot formation*

Soot formation is affected experimentally by two parameters relevant to the present study: water content in the droplet and the initial droplet diameter. Increasing the initial droplet diameter should increase the proportional amount of soot formed. The results presented here for the convection-free environment (and in prior work [1] in the presence of strong convection) indicate a reduction in flame luminosity and sooting as the water content increases in the emulsion drop flame.

Figure 4 shows selected photographs from the motion picture sequences of 0% water droplet (pure heptane), 10% water droplet and a 30% water droplet. The time after ignition is given beneath each photograph. The photographs were obtained under conditions of similar back-lighting and relative motion of the droplet to the camera to facilitate comparing the influence of water. The photographic prints were made of the frame in the series that showed the most intense sooting: note the black "ring" for the heptane droplet. For heptane, the flame is visible and the soot image more intensely shown, though for the emulsion droplets the soot shell is still visible.

Soot aggregates formed during droplet combustion in a low convection environment are trapped between the droplet and flame to form a porous cloud that appears as a "shell" from light scattered where the particle aggregate concentrate. First revealed in photographs reported by Okajima and Kumagai [22], the importance of the soot shell has been discussed in recent years in connection with an influence of initial droplet diameter on the proportional amount of soot formed and the droplet burning rate [5, 11, 18]. If the relative droplet/gas velocity is zero, then the droplet, flame and soot shell should be spherical and concentric. The luminosity of the droplet flames and soot shell configuration show the extent of symmetry of the burning process. The heptane droplet shown in

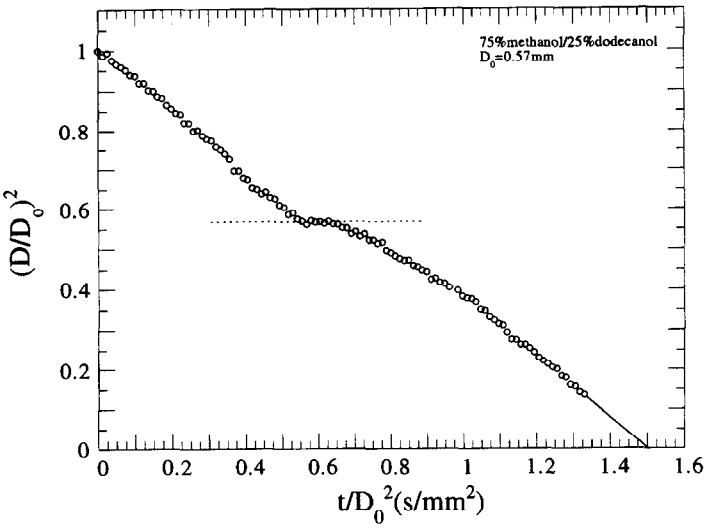

Fig. 3. Variation of normalized droplet diameter $(D/D_o)^2$ with a scaled time (t/D_o^2) for a miscible mixture of methanol and dodecanol which shows a staged burning process (dashed line). Solid line is an extrapolation to the end of burning.

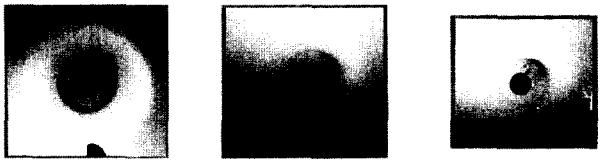

0% water D_0=0.69mm t=0.205s

10% water D_0=0.62mm t=0.165s

30% water D_0=0.74mm t=0.235s

Fig. 4. Selected photographs of unsupported droplets of pure heptane, a 10% water emulsion and a 30% water emulsion droplet. Times after ignition are indicated beneath each image. The soot shell is shown by the dark "ring" and its visibility is most intense for heptane. Photos of the emulsion droplets are of the time when the soot image was darkest for these emulsions (Figs. 5–7 show development of the soot shell). Soot image intensity is reduced for the emulsion droplets compared to heptane.

Fig. 5 closely realizes the idealized process. For the emulsion droplets in Figs. 6 and 7, the larger motion creates a more asymmetric burning pattern.

The effect of water addition on sooting propensity in the combustion of n-heptane is evident in Figs. 4–7. The observed reduction in sooting propensity will increase with increasing liquid water concentration and can be explained by two different yet complementary mechanisms. Firstly, higher concentrations of water vapor between the droplet and the flame will increase the production rate of OH, which is a primary oxidizer of soot precursors. The increased rate of OH production will result in more complete destruction of species which might otherwise lead to soot formation. Secondly, liquid water in the droplet pulls the flame closer to the droplet surface because the water significantly increases the heat of vaporization and thus the gas-phase temperature gradients required at the droplet surface for vaporization. The smaller flame diameter results in lower residence times of fuel molecules inside the pyrolysis zone. The effect of decreased flame sizes on soot precursor species (e.g., acetylene) is predicted by a one-dimensional droplet combustion model which incorporates complex chemistry [23].

Figures 5–7 are a series of photographs for pure heptane (Fig. 5), a 10% water emulsion (Fig. 6) and a 30% water emulsion (Fig. 7). Development of the soot shell is shown for the droplets. Especially evident is the structure of the shell in which aggregates are shown to be drifting outward after a time. Our efforts show that it is difficult to create conditions where the aggregates remain trapped throughout burning. A prior analysis [23] shows that, as the aggregate size increases, the outward Stefan drag force increases more than the inward thermophoretic force, and pushes the aggregates through the flame. In Fig. 5 which shows pure heptane, the shell is intact early in the burning history ($t = 0.205$ s) where also the individual soot aggregate size is very small—too small

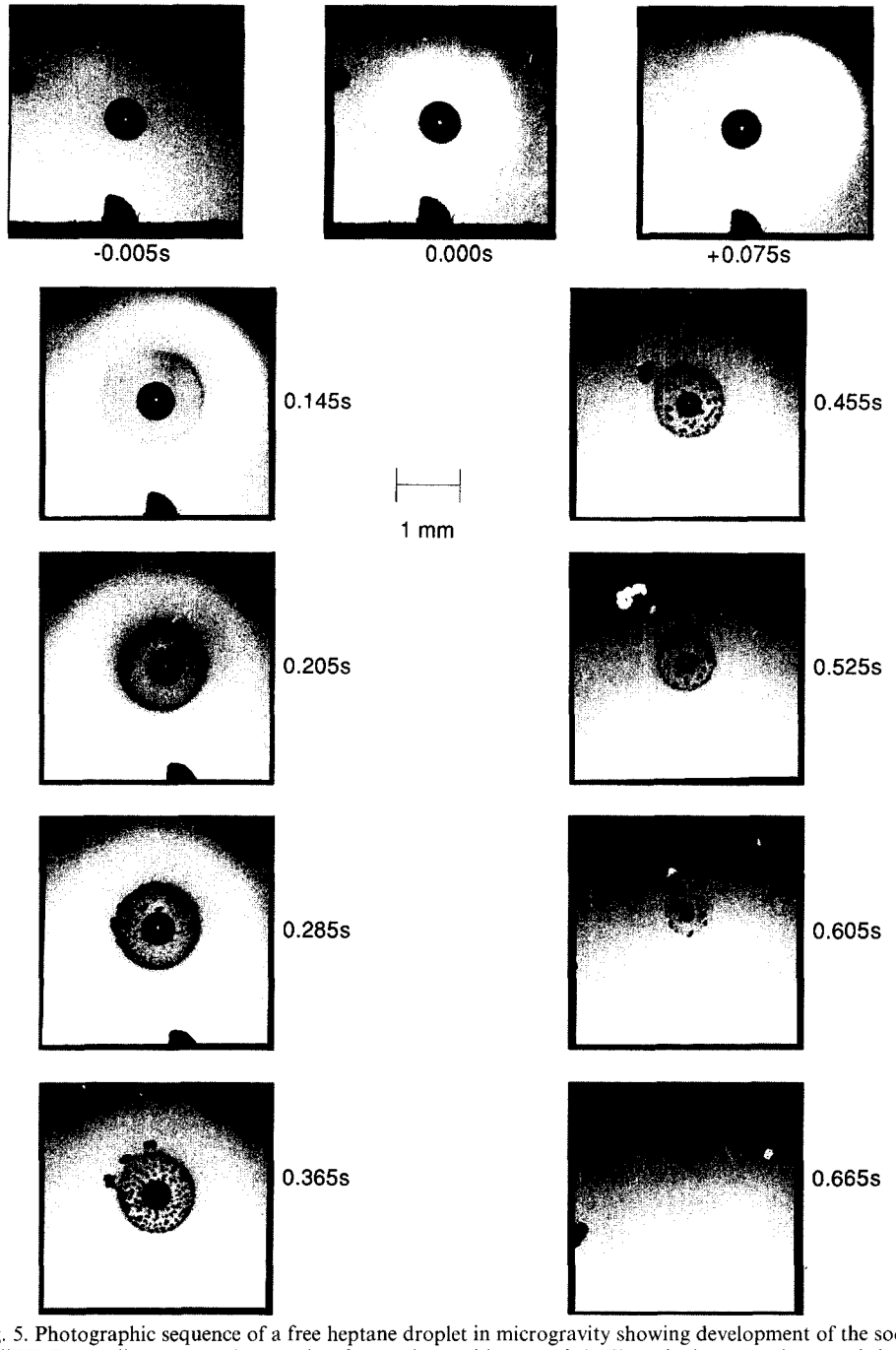

Fig. 5. Photographic sequence of a free heptane droplet in microgravity showing development of the soot shell [5]. Time adjacent to each photo is referenced to ignition ($t = 0$ s). Flame is shown by the outer bright zone, and the soot by the dark ring with black specks (the soot "shell"). Flame visibility decreases as burning progresses and it is not clearly evident after $t = 0.455$ s because of backlighting used to enhance soot visibility. Droplet is still burning as evidenced by white "patch" (upper left at $t = 0.525$ s) which is a soot aggregate that was oxidized as it drifted through the flame.

to be seen with the magnification used. The first evidence of motion of soot particles from the shell is seen at $t = 0.285$ s. At $t = 0.365$ s three large aggregates have clearly separated from the shell. The droplet had almost no perceptible motion for this experimental run which illustrates the sensitivity of aggregate trapping to relative droplet/gas velocity.

For the emulsion droplets (Figs. 6 and 7) which experienced slight relative motion, the soot shell is elongated and develops a "tail" from which the aggre-

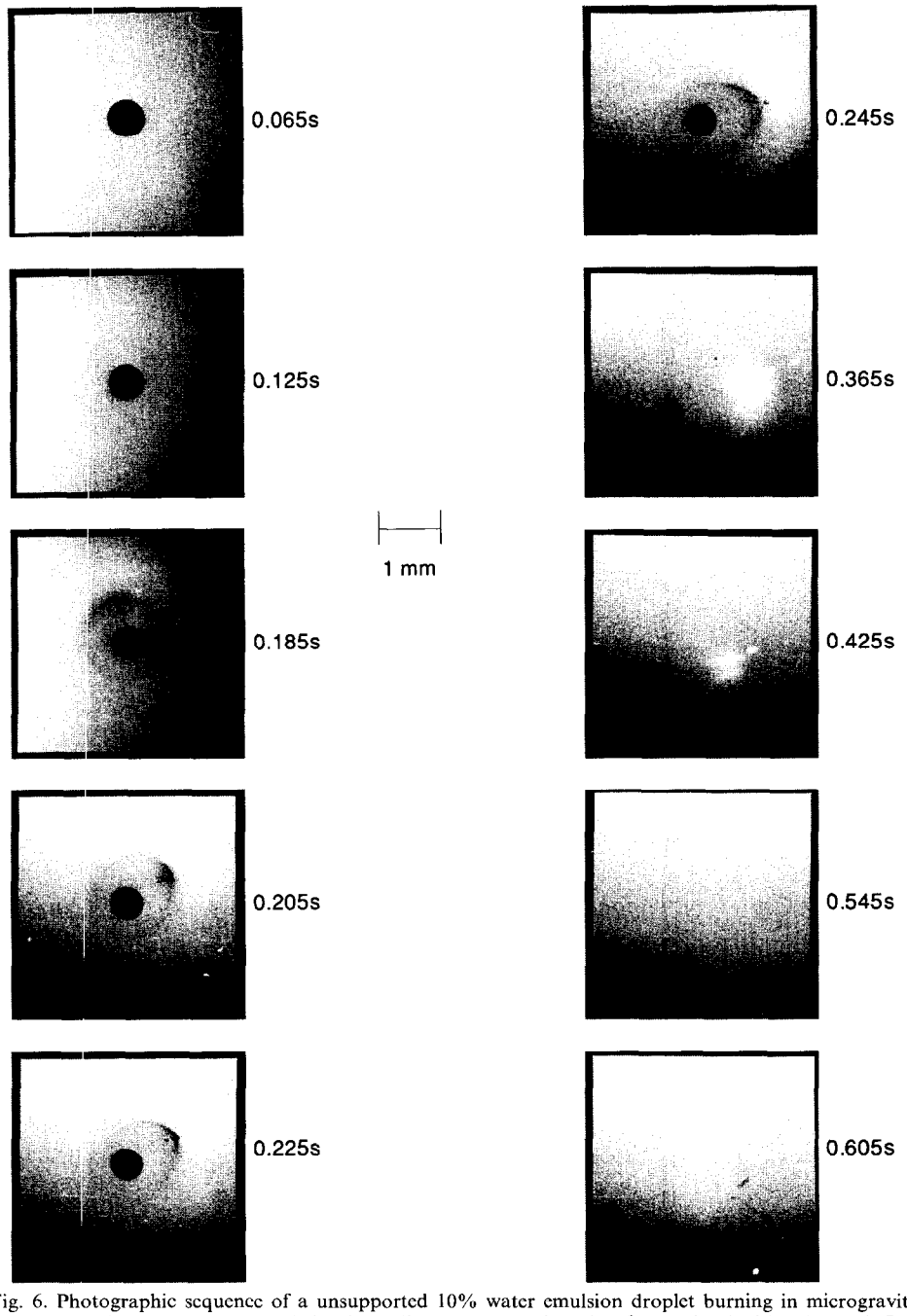

Fig. 6. Photographic sequence of a unsupported 10% water emulsion droplet burning in microgravity showing development of the soot shell. Time adjacent to each photo is referenced to ignition ($t = 0$ s). The spherical soot shell ($t = 0.185$ s) gives way to a nonspherical soot shell ($t = 0.245$ s) due to drift of the droplet. Oxidation of a soot aggregate released from the tip of the shell is shown by the white "flash" at $t = 0.365$ s. Disruption of the droplet occurs at $t = 0.605$ s.

gates pinch off and escape through the flame where they are oxidized. Note, for example, the white "flashes" at $t = 0.365$ s in Fig. 6 and $t = 0.405$ s in Fig. 7. This effect appears to be somewhat typical for microgravity droplet flames due to relative droplet/gas motion. Though the flame (outer luminous zone) is not clearly visible for the sequences in Figs. 6 and 7 (compare with $t = 0.145$ s in Fig. 5 for pure heptane), the emulsion droplets are still burning as evidenced by radiant emission of the soot aggregates that had passed through the reaction zone (the aforementioned "flashes" in Figs. 6 and 7).

4.3. *Bubble nucleation and microexplosion*

Because the water and heptane boiling points are almost identical, bubble nucleation leading to micro-

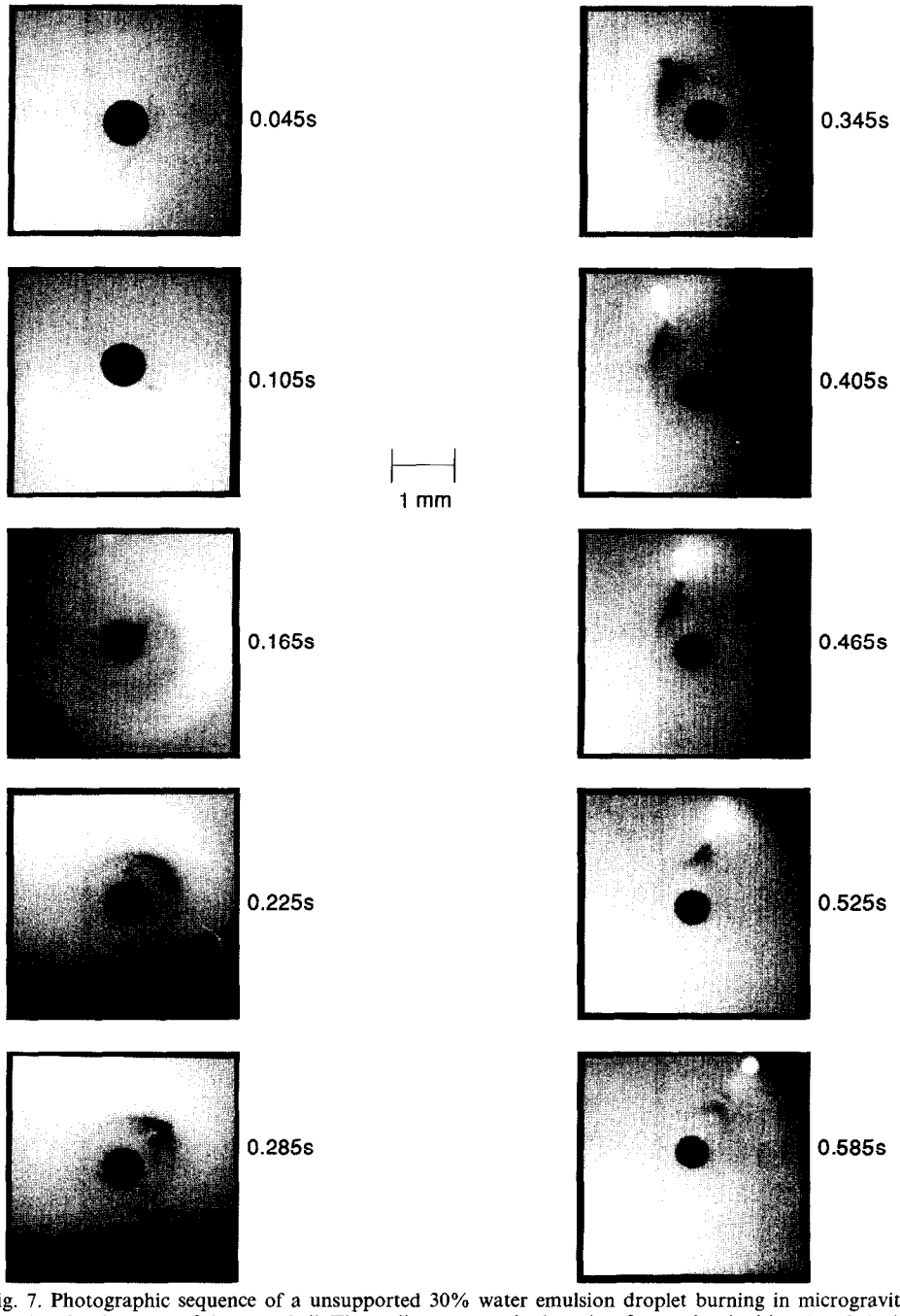

Fig. 7. Photographic sequence of a unsupported 30% water emulsion droplet burning in microgravity showing development of the soot shell. Time adjacent to each photo is referenced to ignition ($t = 0$ s). As with the 10% water emulsion droplet (Fig. 6), white "flashes" (at 0.405 s $< t <$ 0.585 s) are due to oxidation of soot aggregates leaving the shell tip and passing through the reaction zone.

explosion should not have occurred during emulsion droplet combustion. However, it was observed for some of the emulsion droplets and the last frame in Fig. 6 is an example.

The bubble nucleation process within a burning emulsified fuel droplet as originally proposed [24, 25] assumes that a bubble forms at the interface between a trapped water microdroplet and surrounding fuel phase. The corresponding incipient nucleation temperature is higher than the boiling point of either water or heptane, but lower than their respective superheat limits. Because the emulsion droplet temperature cannot exceed the saturation temperature of the fuel phase, bubble nucleation is not theoretically possible

for the water/heptane system by itself. However, the presence of surfactant dissolved in the fuel phase alters this viewpoint.

Because of the surfactant, the emulsion contains not only (nearly) immiscible constituents but *miscible* components (i.e., water with emulsifying agent and heptane with emulsifying agent). The continuous phase is then itself a miscible mixture. Preferential vaporization of the heptane will enrich the droplet surface with the surfactant. Because the surfactant is much less volatile than heptane, the droplet temperature can exceed the boiling point of water when the surfactant begins to dominate vaporization ($t/D_0^2 >$ 1.3 s/mm^2 in Figs. 1 and 2) and bubble nucleation within the droplet then becomes a possibility.

Unlike the microexplosion observed during the burning of methanol/dodecanol droplets in microgravity which occurred in a single event like a balloon bursting [12], the microexplosion of the water-in-heptane emulsion droplets is characterized by a "spitting" event (see Fig. 5) that ejects liquid and partially vaporizes it. This result is also consistent with bubble nucleation near to the droplet surface where the temperature of the droplet is the highest. Bubbles formed at the interface between water microdroplets and surrounding heptane that are near to the emulsion droplet surface would then break through the droplet surface and eject liquid that could conceivably give an effect like that shown in the last frame ($t = 0.605$ s) of Fig. 6.

5. ANALYSIS

A numerical model is used to predict measured emulsion droplet burning rates. The model extends prior analysis on emulsion droplet combustion [2] in the following ways: the flame sheet approximation is relaxed; detailed chemistry at the flame is included rather than assuming a single step global reaction sequence; and temperature and species dependent gas phase property variations are included rather than assuming gas properties are constant. The droplet is assumed to be at the boiling point of the fuel, which is almost the same as that of water. Flame radiation, unsteady gas phase transport processes, and soot formation are not included so that the results are more applicable to the emulsion droplets that were found to soot proportionally less than heptane. Ignition is assumed to occur instantaneously from a spherical source surrounding the droplet. This assumption is only very approximately approached in the experiment with the two spark ignition design, but is still more symmetric than using a single spark ignition set-up. Finally, the emulsion droplet composition is assumed to be "frozen" because this assumption is the only one that is consistent with that of a spherically symmetric burning process in which the droplet interior should theoretically be motionless. Below, we discuss which of the three stages discussed in Section 4.1 is best predicted by the model.

The 96-step complex chemistry scheme of Warnatz [26] is used for heptane. More complex mechanisms for heptane exist, such as the 659-step sequence of Lindstedt and Maurice [27], but the temperature distribution and profiles of major combustion species such as CO_2, H_2O, and CO are not expected to be strongly effected by the reaction pathways to oxidation, because of the good agreement obtained between experiments on counterflow diffusion flames and modelling by Bui-Pham and Seshadri [28] with the mechanism developed by Warnatz [26]. The distribution of secondary species such as acetylene (C_2H_2) may, however, depend on the reaction mechanisms but they are not of interest for the present study because soot formation is neglected, in keeping with the observed reduced sooting for the emulsions.

More important, we believe, for the present purposes, is correctly accounting for the temperature and species' influences on physical properties. Gas phase properties are evaluated from Coffee and Heimerl [29] and Kee *et al.* [30], and specific heats and enthalpies are taken from the CHEMKIN data base [31]. Liquid property values are taken from the data base of Vargaftik [15]. The governing equations are the one-dimensional species, energy and overall mass conversation equations. Details of the numerical procedures are discussed elsewhere [23]. Results are shown by the lines in Figs. 1 and 2.

The predicted evolution of droplet diameter shown in Figs. 1 and 2 (the solid line) has a single burning rate due to the frozen assumption used in the model. Comparing the lines in Figs. 1 and 2 with the data show that the stage 2 burning rate for the emulsion droplets is most closely aligned with the predicted values. Figure 8 is a cross-plot that compares predicted and measured stage 2 burning rates. The initial droplet diameter for the calculation did not influence the burning rate (because of the neglect of radiation and soot formation in the model) and a value of 0.6 mm was used. The agreement is good for the emulsions which suggests that the combustion mode for stage 2 is indeed "frozen". The burning rate for heptane is not well predicted because soot formation and radiation are neglected in the model both of which can be important for the more highly sooting heptane droplet flame compared to the emulsions (see Fig. 4).

Stage 1 can be considered as a delay period to the stage 2 frozen combustion mode. A mechanism for such a delay period is conjectured in which a layer of heptane/surfactant mixture in the emulsion droplet surrounds the embedded water microdroplets like a "skin". During the time that the surface is regressing to where the water microdroplets are first exposed to the gas, little water evaporates. When the surface reaches the periphery of the water microdroplets in the emulsion, the water microdroplets are uncovered and start to evaporate and initiate the frozen evaporation mode of stage 2.

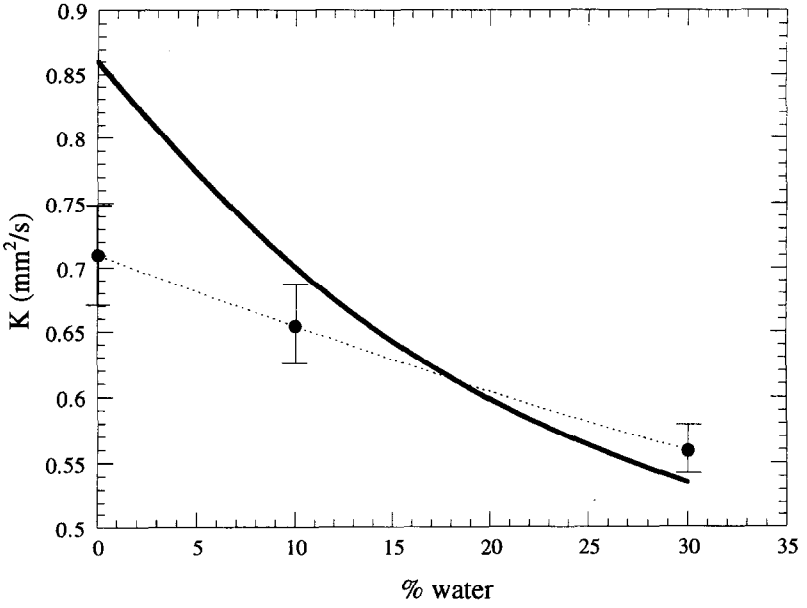

Fig. 8. Variation of burning rate with water volume percent. Solid line is a prediction from the numerical analysis which assumes a "frozen" combustion mode. Data points are stage 2 burning rates for the emulsion droplets (see Figs. 1 and 2). Dashed line through the measurements is a trend line.

6. CONCLUSIONS

The results of these unsupported water/heptane emulsion droplet experiments carried out in a low convection environment are the following:

(1) Emulsification of heptane with water reduces the droplet flame luminosity and soot formation. Soot collects in a shell-like structure similar to single component fuel burning in a convection-free environment.

(2) A staged burning process occurs for the emulsions in which heptane (stage 1), then both heptane and water (stage 2), and finally surfactant (stage 3) control the burning process. A period of constant diameter due to droplet heating occurs between stages 2 and 3, because of the large differences in boiling point between water and heptane on the one hand, and surfactant on the other.

(3) In the final stage of burning, the transition to surfactant-dominated vaporization terminates by microexplosions. Microexplosions are observed even though the heptane and water boiling points are almost identical. This result is attributed to enrichment of the surfactant concentration at the droplet surface during the burning history which would raise the droplet temperature above that required for bubble nucleation within the emulsion.

(4) Measured stage 2 burning rates are in good agreement with predicted values, so it appears that the emulsion composition is "frozen" during stage 2.

Acknowledgements—The authors are grateful for the financial support provided by the National Aeronautics and Space Administration, NAG3-1791, and in the earlier stages of our work on droplet combustion processes by the New York State Center for Hazardous Waste Management. The authors appreciate the help of Prof. F. D. McLeod, and Messrs R. Shah and Brian Callohan.

REFERENCES

1. Jahani, H. and Gollahalli, S. R., Characteristics of burning jet A fuel and jet A fuel–water emulsion sprays. *Combustion and Flame*, 1980, **37**, 145–154.
2. Law, C. K., Lee, C. H. and Srinivasan, N., Gas-phase combustion characteristics of water-in-oil emulsion droplets. *Combustion and Flame*, 1980, **37**, 125–143.
3. Lasheras, J. C., Fernandez-Pello, A. C. and Dryer, F. L., Initial observations on the free droplet combustion characteristics of water-in-fuel emulsions. *Combustion Science and Technology*, 1979, **21**, 1–14.
4. Glassman, I., Comments, *16th Symposium (International) on Combustion*. The Combustion Institute, Pittsburgh, 1977, pp. 303–304.
5. Jackson, G. S. and Avedisian, C. T., Experiments on the effect of initial diameter in spherically symmetric droplet combustion of sooting fuel. *Proceedings of the Royal Society of London*, 1994, **A446**, 255–276.
6. Okajima, S., Kanno, H. and Kumagai, S., Combustion of emulsified fuel droplets under microgravity. *Acta Astronautic*, 1985, **12**, 555–563.
7. Kimura, M., Ihara, H., Okajima, S. and Iwama, A., Combustion behaviors of emulsified hydrocarbons and JP-4/N_2H_4 droplets at weightless and free falling conditions. *Combustion Science and Technology*, 1986, **44**, 289–306.
8. Tuse, M., Segawa, D., Kadota, T. and Yamasaki, H., Observation of sooting behavior in an emulsion droplet flame by planar laser light scattering in microgravity. *26th Symposium (International) on Combustion*. The Combustion Institute. Pittsburgh, 1996, pp. 1251–1258.

9. Tuse, M., Segawa, D., Yamasaki, H. and Kadota, T., Effects of fuel properties and water contents on micro-explosion behavior of an emulsified fuel droplet under microgravity. *Proceedings of the 12th International Symposium on Space Technology*, 1994, pp. 1000–1005.
10. Avedisian, C. T., Yang, J. C. and Wang, C. H., On low gravity droplet combustion. *Proceedings of the Royal Society of London*, 1988, **A420,** 183–200.
11. Jackson, G. S., Avedisian, C. T. and Yang, J. C., Observations of soot in droplet combustion at low gravity: heptane and heptane/monochloroalkane mixtures. *International Journal of Heat and Mass Transfer*, 1992, **35,** 2017–2033.
12. Yang, J. C., Jackson, G. S. and Avedisian, C. T., Combustion of unsupported methanol/dodecanol mixture droplets at low gravity. *23rd Symposium (International) on Combustion*. The Combustion Institute, Pittsburgh, 1990, pp. 1619–1625.
13. Sirignano, W. A., Fuel droplet vaporization and spray combustion theory. *Progress in Energy and Combustion Science*, 1983, **9,** 291–322.
14. Pal, R. and Rhodes, E., Viscosity/concentration relationships for emulsions. *Journal of Rheology*, 1989, **33,** 1021–1045.
15. Vargaftik, N. B., *Handbook of Physical Properties of Liquids and Gases*, 2nd edn. Hemisphere Publishing Co., New York, 1975.
16. Schlichting, H., *Boundary Layer Theory*, 6th edn. McGraw-Hill, New York, 1968, p. 106.
17. Yang, J. C., An experimental method for studying combustion of an unsupported fuel droplet at reduced gravity, Ph.D Thesis, Cornell University, 1990.
18. Avedisian, C. T., Soot formation in spherically symmetric droplet combustion, *Combustion Science and Technology and Technology Book Series*, Vol. 4. Gordon and Breach Publishers, 1997, pp. 135–150.
19. Avedisian, C. T. and Fatehi, M., An experimental study of the Leidenfrost evaporation characteristics of emulsified liquid droplets. *International Journal of Heat and Mass Transfer*, 1988, **31,** 1587–1603.
20. Wang, C. H., Combustion and microexplosion on multicomponent droplets, Ph.D Thesis, Northwestern University, 1983.
21. Glassman, I., *Combustion* 2nd edn. Harcourt, Brace, Jovanovich, Orlando, 1987, p. 271.
22. Okajima, S. and Kumagai, S., Further investigations of combustion of free droplets in a freely falling chamber including moving droplets. *15th Symposium (International) on Combustion*. The Combustion Institute, Pittsburgh, 1975, pp. 401–407.
23. Jackson, G. S. and Avedisian, C. T., Modelling of spherically symmetric droplet flames including complex chemistry: effect of water addition on *n*-heptane droplet combustion. *Combustion Science and Technology*, 1996, **115,** 127–147.
24. Avedisian, C. T. and Andres, R. P., Bubble nucleation in superheated liquid–liquid emulsions. *Journal of Colloid and Interface Science*, 1978, **64,** 438 453.
25. Avedisian, C. T., Nucleation at a liquid–liquid interface and exploding drops in emulsified fuel combustion, Report No. 1315. Department of Mechanical and Aerospace Engineering, Princeton University, Princeton, NJ, 1976.
26. Warnatz, J., Chemistry of high temperature combustion of alkanes up to octane. *20th Symposium (International) on Combustion*. The Combustion Institute, Pittsburgh, 1977, pp. 845–856.
27. Lindstedt, R. P. and Maurice, L. Q., Detailed kinetic modelling of *n*-heptane combustion. *Combustion Science and Technology*, 1995, **107,** 317–353.
28. Bui-Pham, M. and Seshadri, K., Comparison between experimental measurements and numerical calculations of the structure of heptane–air diffusion flames. *Combustion Science and Technology*, 1991, **79,** 293–310.
29. Coffee, T. P. and Heimerl, J. M., Transport algorithms for premixed laminar steady state flames. *Combustion and Flame*, 1981, **43,** 273–289.
30. Kee, R. J., Dixon-Lewis, G., Warnatz, J., Coltrin, M. E. and Miller, J. A., A FORTRAN computer code package for the evaluation of gas-phase multicomponent transport properties. Sandia National Laboratories, SAND86–8246, 1986.
31. Kee, R. J., Rupley, F. M. and Miller, J. A., The CHEMKIN thermodynamic database. Sandia National Laboratories, SAND87-8215B, 1987.